Combined Inverse Fourier Transformation of Magnetic Resonance and Intensity-Curvature Functional Images

Carlo Ciulla

Department of Computer Engineering,
Epoka University,
Rr. Tiranë-Rinas, Km. 12, 1032
Vorë, Tirana, Albania.
Email: cciulla@epoka.edu.al; cxc2728@njit.edu
ORCID ID: https://orcid.org/0000-0002-5563-6036

Abstract

This research reports on an image processing technique used to merge Magnetic Resonance Imaging (MRI) or Magnetic Resonance Angiography (MRA) with their intensity-curvature functional (ICF). Given a two-dimensional MR image, six 2D model polynomial functions were fitted to the image, and six ICF images were calculated. The MR image and its ICF were direct Fourier transformed. The phase of MR image was estimated pixel-by-pixel as arctangent of ratio between imaginary and real components of k-space and is called phase ratio. The phase of ICF is the phase of inverse Fourier transformation and is called base phase. The two values of phase were summed up and used to reconstruct ICF images through inverse Fourier transformation. The reconstructed image is the combination of MR and ICF. Data obtained with T2-MRI and MRA indicates that the technique improves vessel detection in T2-MRI and contrast enhances T2-MRI and MRA.

Running Head: MRI-ICF Fusion

Keywords: intensity-curvature functional, magnetic resonance imaging, inverse Fourier transformation, base phase, phase ratio.

Introduction

1. Vessels imaging, detection and contrast enhancement through MRI

Human brain vessel imaging is customarily performed using magnetic resonance angiography (MRA), magnetic resonance imaging (MRI), computed tomography (CT), ultrasound (US) with color Doppler [1], high-resolution intracranial vessel wall MR imaging (IVW-MR imaging), and computed tomographic angiography (CTA) [2]. Within the aforementioned array of choices, MRA remains the modality which serves as the most important and primary diagnosis tool. MRA scans are used to find the first remarkable evidence of pathology and also to elucidate and/or

confirm the clinical condition of patients, before investigating further the patient with MRI. Indeed, high resolution-MRI is used in combination with T1-weighted [3], T2-weighted protocols, proton density imaging and contrast enhanced T1-weighted MRI [1]. T2-weighted MRI is also used in combination with susceptibility weighted imaging (SWI) [4]. FLAIR pre and post contrast agent injection is used in conjunction with T1 and T2-MRI [5]. In the past fifteen years SWI-based MR venography has gained momentum and is now considered as one of the leading MR techniques used to image the vasculature of the human brain [6]. On the basis of SWI current trends have progressed to calculation of susceptibility maps which is also an instrument for the creation of human brain venograms [7, 8]. Human brain vessel detection is relevant to relative orientation between vessel and magnetic field and also relevant to vessel intrinsic magnetic susceptibility (which determines the MRI signal). Brain magnetic susceptibility has been demonstrated to be anisotropic while introducing the computational technique called susceptibility tensor imaging (STI) [9]. Feasible ways to enhance vessels detection and contrast enhancement in MRI include: 1. Use of contrast agent injection [10]. 2. Use of ultra or very high magnetic fields because of enhanced susceptibility effects in the vasculature territory [11], Or like SWI: 3. Use of the properties of paramagnetic deoxyhemoglobin which causes contrast between the vessels and the surrounding tissues [12].

2. The proposed technique

The intensity-curvature functional is a property of the model polynomial function. An immediate application of intensity-curvature functional is re-sampling which yields to the ICF image. The ICF image has been proposed as image space and k-space filter in MRI [13-15]. To calculate the ICF of the model function requires the model polynomial function to be second order differentiable and to have non null sum of second order partial derivatives calculated at the origin of the pixel coordinate system. The visual appearance of ICF is high pass filtered signal and ICF of T2-weighted MRI of the human brain yields information about the vasculature [13]. The motivation of this research is to improve vessels details detection and contrast enhancement in Magnetic Resonance of the human brain. Two techniques were chosen among the MR spectrum. T2-weighted MRI, which is not indicated for vessels detail detection, and MRA which is among the best techniques for vessels imaging. The purpose of this paper is to report a technique that merges MR image and ICF image. MR image and its ICF are Fourier transformed. The phase of the MR image is calculated pixel-by-pixel as the arctangent of ratio between imaginary and real components of k-space and is called phase ratio. The ICF is inverse Fourier transformed using as phase the sum of: 1. The phase of MR image (phase ratio), and 2. The

phase of ICF. The phase of ICF is the phase of the direct Fourier transformation and is called base phase. Merging MR and ICF is determined through reconstruction with inverse Fourier transformation of ICF using as phase the sum of base phase and phase ratio. The combination MR and ICF is called reconstructed image. This research shows that comparing reconstructed image with MR, in either of the two cases: T2-MRI and MRA; an improvement is possible, which is vessels details detection and contrast enhancement.

Methods and Materials

T2-weighted MRI images were acquired from 10 healthy subjects. An additional MR angiography from another subject was included in the study. MRI acquisition was consented and approval was obtained from subjects to use the images for research after the administration of written consent. MRI images were fitted with six model polynomial functions: 1. Bivariate cubic, 2. Bivariate Lagrange (two different functions), 3. Bivariate quadratic B-Spline, 4. Bivariate cubic B-Spline, 5. Bivariate linear. The mathematics of the model polynomial functions were reported elsewhere while describing the intensity-curvature functional calculated from MRI [13-15]. Table 1 shows the abbreviations used in this manuscript when referring to model polynomial functions [13-15].

Model Polynomial Function	Bivariate cubic	Bivariate cubic Lagrange	Bivariate quadratic B-Spline	Bivariate cubic B-Spline	Bivariate cubic Lagrange	Bivariate Linear
	B32D	G42D	H32D	H42D	LGR2D	SRE2D

Table 1. The abbreviations of the model polynomial functions.

T2-MRI and MRA images were used to calculate their ICFs (one for each model polynomial function) and they were Fourier transformed. The ICFs were also Fourier transformed. The inverse Fourier transform used two values of the phase. The base phase which is the phase used commonly for Fourier transformations. And, the phase ratio, which was calculated using the arctangent of the ratio between imaginary and real components of MR k-space. The inverse Fourier transformation of the ICF used the sum of these two values of the phase to accomplish to calculate the reconstructed image. The reconstructed image is the combination of MR and ICF. Figure 1 illustrates the aforementioned process.

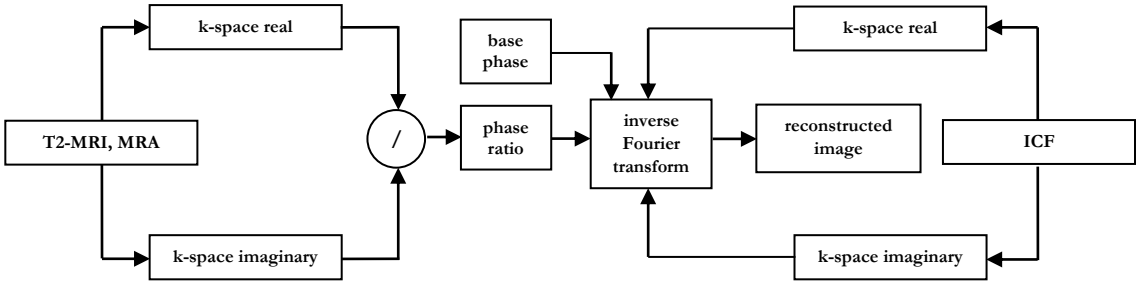

Fig. 1 The signal processing technique used to merge MR with ICF of MR.

	T2-MRI	reconstructed image: merged MR & ICF
MRA	-	check for contrast enhancement
reconstructed image: merged MR & ICF	check for improved vessel detection	-

Table 2. The comparisons between images.

As shown in Table 2, the reconstructed image was compared to T2-MRI: 1. to check for improved vessel detection and to MRA: 2. to check for contrast enhancement. Note that the comparison of the ICF and MRI was reported elsewhere [13, 16]. Table 3 reports the acquisition parameters of the MR acquisitions.

Parameters	**MRI acquisition**	**MRA acquisition**
TE (Time to Echo)	96 msec	6.9 msec
TR (Repetition Time)	4720 msec	48 msec
FOV (Field of View)	204 x 250	230 x 230
pixel matrix size	262 x 320	512 x 512
# of slices	28	15

Table 3. MRI & MRA acquisition parameters

Theory

Let $f(i,\ j)$ be the pixel intensity of MR image and ICF image. The direct discrete Fourier transformation yields the real and imaginary components $Re(i,\ j)$ and $Im(i,\ j)$ of the k-space as:

$$Re(i,\ j) = \sum_{i=0}^{N_x} \sum_{j=0}^{N_y} f(i,\ \ j) \cdot (\cos\varphi + \sin\varphi) \tag{1}$$

$$Im(i,\ j) = \sum_{i=0}^{N_x} \sum_{j=0}^{N_y} f(i,\ \ j) \cdot (-\sin\varphi + \cos\varphi) \tag{2}$$

The base phase is:

$$\varphi = \frac{2.0\ \pi\ i\ j}{N_x N_y} \tag{3}$$

Where x and y are the spatial coordinates of the image. N_x, N_y are the number of pixels of the image along x and y directions respectively. Let the imaginary and real components of the k-space of MR be defined by $Re_{MR}\ (i,\ j)$ and $Im_{MR}(i,\ j)$ and they are calculated with equations (1) and (2) respectively. The phase ratio is φ_1:

$$\varphi_1 = \frac{2.0\,\pi \cdot atan2(\,Im_{MR}(i,j),\ \ Re_{MR}\,(i,j)\,)}{N_x N_y} \tag{4}$$

The phase ratio is summed to the base phase φ. The sum is the phase ω as per equation (5).

$$\omega = \ \varphi + \varphi_1 \tag{5}$$

ω is used to inverse Fourier transform the combination of MR and ICF which is indicated in equations (6) and (7). ω varies on a pixel-by-pixel basis. Let $Re_{ICF}\ (i,\ j)$ and $Im_{ICF}\ (i,\ j)$ be the real and imaginary components of the k-space of the ICF calculated with the direct discrete Fourier transformation as per equations (1) and (2). The real and imaginary components of the reconstructed image are:

$$Real(i,\ j) = \ \sum_{i=0}^{N_x} \sum_{j=0}^{N_y} Re_{ICF}\ (i,\ j) \cdot (\cos\omega + \sin\omega) \tag{6}$$

$$Imaginary(i,\ j) = \ \sum_{i=0}^{N_x} \sum_{j=0}^{N_y} Im_{ICF}\ (i,\ j) \cdot (-\sin\omega\ +\ \cos\omega) \tag{7}$$

$$g(i,\ \ j) = \ \sqrt{Real(i,\ j)^2 + Imaginary(i,\ j)^2} \tag{8}$$

The coefficients $(\cos\omega + \sin\omega)$ and $(-\sin\omega\ +\ \cos\omega)$ embed the characteristics of the k-space of MR. The result of inverse Fourier transform is reconstructed image pixel $g(i,\ \ j)$ as per equation (8).

Results

1. The need of the base phase

Figure 2 illustrates the need of the base phase for the implementation of the signal processing technique reported in this paper. The base phase is presented in (C) and (C1) and its k-space is shown in (H) and (H1) respectively. The phase of images in (A) and (A1) is calculated as ratio of imaginary and real components of the k-space and is presented in (D) and (D1).

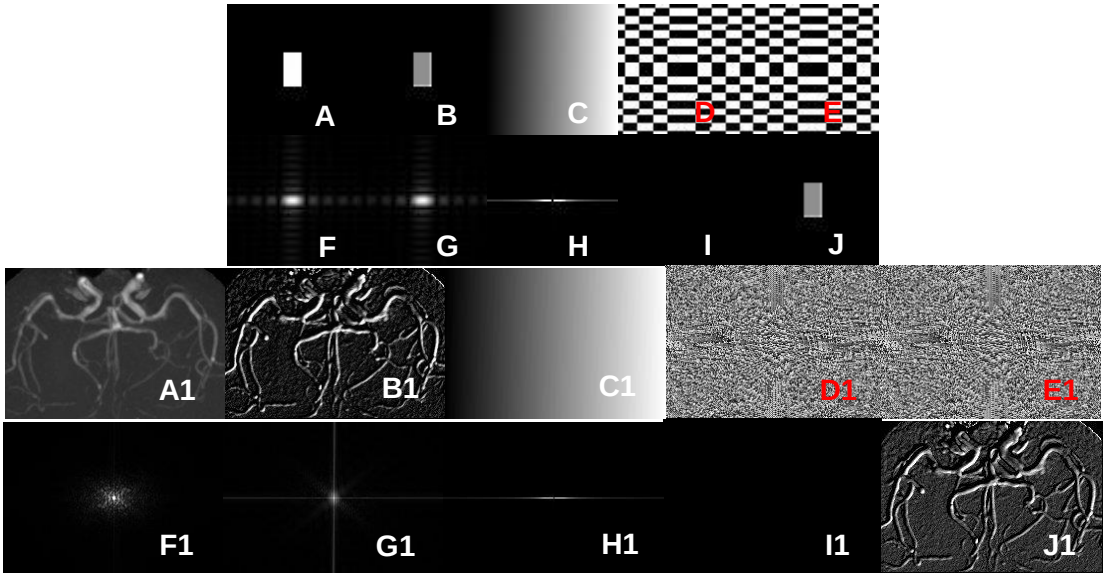

Fig. 2 Rectangle image in (A) and MRA in (A1). ICF calculated with the SRE2D model polynomial in (B) and (B1). Base phase in (C) and (C1). (D) and (D1) Phase as ratio of imaginary and real components of the k-space of (A) and (A1). (E) is the sum of (C) and (D), (E1) is the sum of (C1) and (D1). (F) and (F1) k-space magnitude of (A) and (A1). (G) and (G1) k-space magnitude of (B) and (B1). (H) and (H1) k-space magnitude of (C) and (C1). (I) and (I1) reconstructed image making no use of the base phase. (J) and (J1) reconstructed image making use of the phase sum ((C) plus (D), for (J); and (C1) plus (D1), for (J1)).

As shown in (I) and (I1), the inverse Fourier transformation fails if base phase is not used for signal reconstruction. When the base phase is summed to phase ratio as displayed in (E) and (E1), the inverse Fourier transformation is successful and the reconstructed signal is shown in (J) and (J1). Clearly the ICF seen in (B) and (B1) is not the same as the reconstructed signal shown in (J) and (J1), which is combination of signal (see (A) and (A1)) and ICF of signal (see (B) and (B1)). Note that numerical value of base phase is considerably smaller than numerical value of phase ratio and so the images in (D) and (E) appear very similar. Likewise for (D1) and (E1).

2. The reconstructed image versus ICF and MR

Figures 3 and 4 present the evidence that there is an advantage of the reconstructed image (merge of MR and ICF) versus MR. The reconstructed images display more richness of details in reference to the vessels and also contrast enhancement versus MR. This is a recurring occurrence and this evidence is presented in support of the significance of the proposed image processing technique.

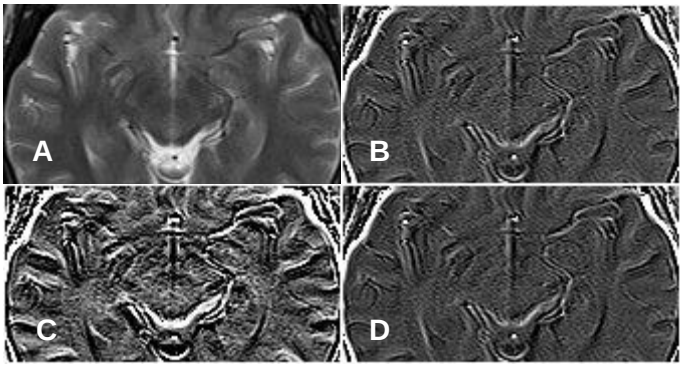

Fig. 3 T2-MRI in (A). ICF calculated with H42D in (B). (C) Reconstructed image through inverse Fourier transform of (A) and (B). (D) Difference image between (B) and (C).

Figure 3 shows T2-weighted MRI (see (A)), and reconstructed image obtained through inverse Fourier transformation of the combination of MR and ICF (see (B)). The reconstructed image presents details of the vessel structures yet discernible in T2-MRI. Moreover, reconstructed image show improved vessels details detection and contrast enhancement when compared to MR in (A).

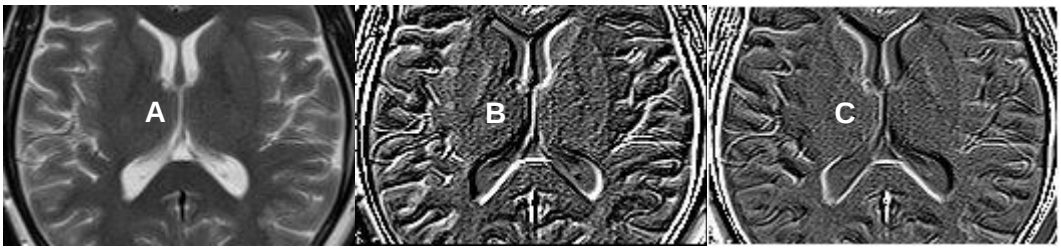

Fig. 4 T2-MRI in (A). (B) Inverse Fourier transformed k-space merge of (A) and SRE2D ICF of (A). (C) Inverse Fourier transformed k-space merge of (A) and H42D ICF of (A). SRE2D ICF is calculated fitting MRI with SRE2D. H42D ICF is calculated fitting MRI with H42D. The images in (C) and (D) improve vessels details detection versus the MR image and also contrast enhance the vessels discernible in the T2-MRI.

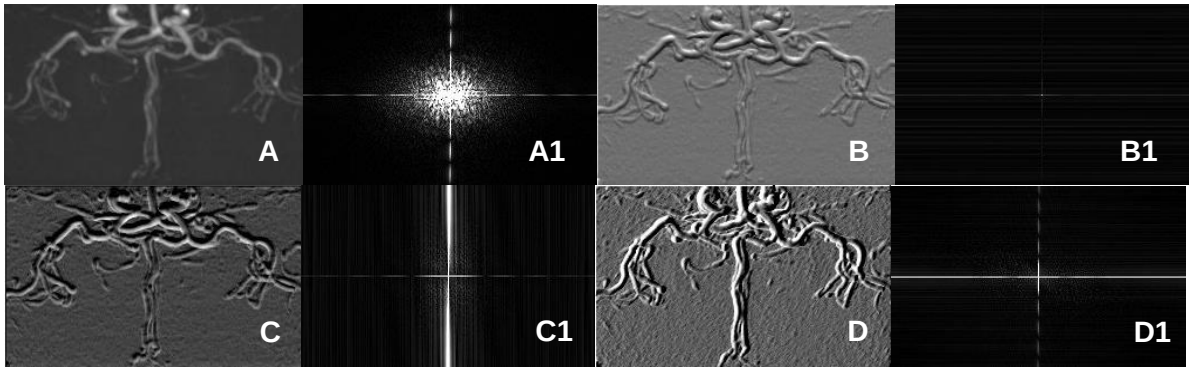

Fig. 5 Magnetic Resonance Angiography (MRA) in (A). G42D ICF merged with MRA in (B), H32D ICF merged with MRA in (C), LGR2D ICF merged with MRA in (D). k-space of the images in (A) through (D) is labelled (A1) through (D1).

Figure 5 presents results of obtained using MRA (see (A)) as departing image. Sharpening, increases the contrast and so it makes vessels more perceptible versus the background signal (compare for instance (B), (C), (D) with (A)). As result, the reconstructed images provide different brightness contrast enhancement when compared to MRA. This aspect confirms what already seen for T2-MRI in Figures 3 and 4. Finally, k-space images in Figure 5 provide qualitative account of the reconstructed images. The similarities of results obtainable through ICF and reconstructed image is illustrated in Figure 6 where an MRA case is analyzed. Figure 6 looks at the similarities of ICF and reconstructed image from two perspectives: image and image edge finding properties. The image edge finding properties are displayed for MRA in (D), ICF in (E) and reconstructed image in (F).

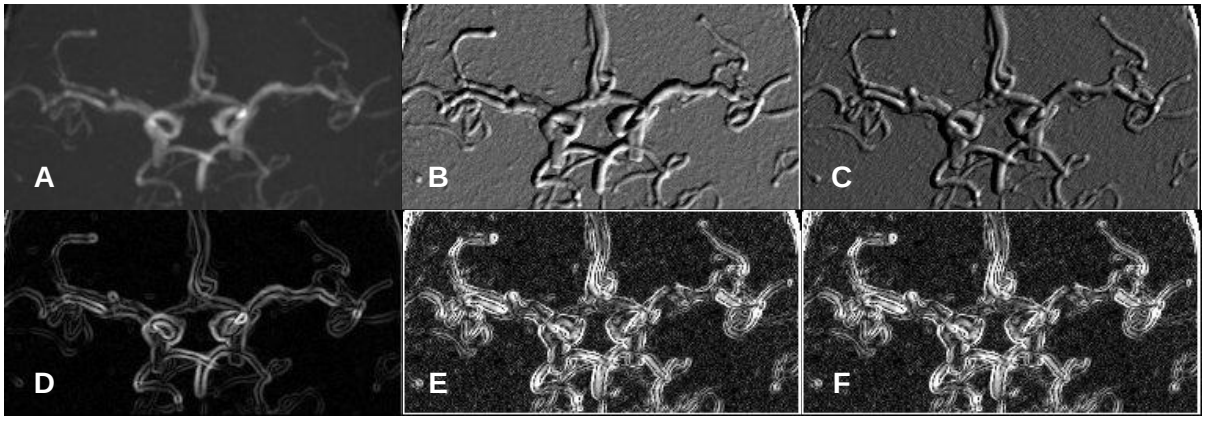

Fig 6 MRA in (A). ICF calculated with B32D in (B). (C) Reconstructed image obtained merging (A) and (B). First order derivative images of (A), (B) and (C) are presented as edge finders in (D), (E) and (F), respectively. The first order derivatives were calculated using the bivariate linear model function SRE2D [17].

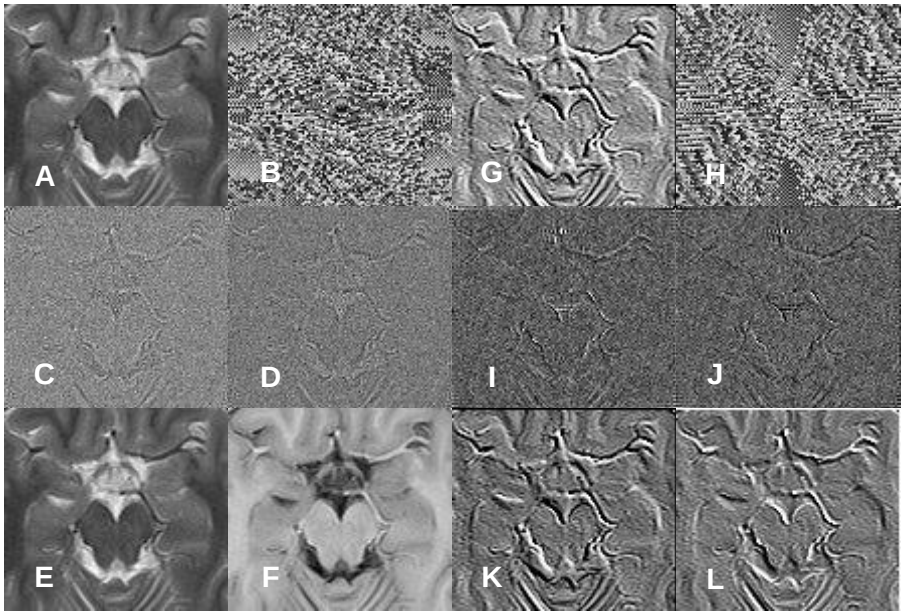

Fig. 7 T2-MRI in (a). Phase ratio of T2-MRI in (b). (c) Real component of k-space of (b). (d) Imaginary component of k-space of (b). Reconstructed T2-MRI in (e). (g) ICF of T2-MRI calculated with SRE2D model polynomial function. (h) Phase ratio of ICF. (i) Real component of k-space of (h). (j) Imaginary component of k-space of (h). The image in (e) results from the inverse Fourier transformation of the sum of k-space of T2-MRI and k-space of phase ratio. The image in (k) results from the inverse Fourier transformation of the sum of k-space of ICF and k-space of phase ratio. The image in (f) is difference between T2-MRI (a) and reconstructed T2-MRI (e). The image in (l) is difference between ICF of T2-MRI (see (g)) and reconstructed ICF of T2-MRI (see (k)).

To ascertain the meaning of phase ratio and to validate its use in the image processing technique proposed in this paper, Figure 7 shows in (b) phase ratio of T2-MRI (see (a)), k-space real and imaginary components of phase ratio in (c) and (d) respectively. Figure 7 also shows in (e) T2-MRI reconstructed inverse Fourier transforming the sum of k-space of T2-MRI and k-space of phase ratio. The image in (f) is difference between images in (a) and (e) and such difference gives meaning to phase ratio. Figure 7 also shows ICF of T2-MRI in (g), phase ratio of ICF in (h), k-space real and imaginary components of phase ratio in (i) and (j). Figure 7 finally shows in (k) ICF reconstructed inverse Fourier transforming the sum of k-space of ICF and k-space of the phase ratio. Note the difference between (l) and (g), (k), and this difference validate the use of phase ratio in the here proposed image processing technique. The image in (l) is difference between images in (g) and (k).

In summary, phase ratio embeds vessel information which is used inverse Fourier transforming the sum of k-space of ICF and k-space of phase ratio, so to obtain images like (k). The difference image in (l) reveals that ICF and reconstructed ICF are not equal.

Discussion and Conclusion

1. The image processing technique

The present research relates to vessel imaging, it looks at the computational aspect and is motivated by recent developments [13-16], which indicate intensity-curvature functional of MR images as filtering technique able to achieve vessel detection and contrast enhancement. Hence, this paper proposes a novel fully computational technique which explores the combination of MR images with ICF images. The technique is based on inverse Fourier transformation of k-space of ICF using as phase the sum of base phase and phase ratio. The base phase is the phase used normally when direct or inverse Fourier transforming the image. The phase ratio is the arctangent of the ratio between imaginary and real component of the k-space of the MR image. The phase ratio is thus the numerical parameter used to merge k-space of ICF with k-space of MR. Reconstructed images are similar to ICF and when compared to the departing MR offer level of detail of the vessel structures that are not overtly observable in T2-MRI. Moreover, the contrast enhancement offered by reconstructed images is additive to the invaluable information already provided by MRA. As recently reported, the ICF was used as k-space filter [13, 16] subtracting the k-space of the ICF from the k-space of MR, and inverse Fourier transforming back the subtraction signal. In this paper a new approach is undertaken. The approach takes into account MR through a measure (phase ratio) and embeds this measure into formulation (see equations (6), (7)) merging k-space of ICF and k-space of MR.

2. Novel contribution

The contribution of this paper to the state of the art is two folded. One is the computational technique used to reconstruct ICF after fusing it with the k-space of MR data. The other one is to be able to extract, visualize and contrast enhance vessels imaged with T2-weighted MRI. T2-weighted MRI is not indicated for vessel imaging, and in this context, the paper proposes a technique able to improve vessels detail detection in T2-MRI. This aspect is not reported elsewhere and it is thus the main novelty of this research versus recent developments [13-16]. Moreover, this research makes a neat progress versus the inverse Fourier transformation procedure reported earlier [14]. The present technique consists of merging two images in k-space using phase (see Fig. 1), while previous research [14] inverse Fourier Transform the difference

between k-space of MRI and k-space of intensity-curvature-term (compare Fig. 1 with Table 3 in [14]). In other words, the present technique encodes MRI phase (called phase ratio) into ICF phase (called base phase) and inverse Fourier transforms into reconstructed ICF (which embeds MRI information in it), thus fusing ICF and MR image. The reproducibility of results of the present technique is assured by rigorous mathematical methodology adopted for Fourier based signal reconstruction and using calculus for ICF calculation.

3. Context and literature

The context of this research is human brain vessels imaging, which is nowadays performed with a combination of large arrays of MR based imaging techniques. In fact, recent trends in research and the parallel introduction of high and ultrahigh field MR scanners indicate intracranial vessel wall MR imaging to be among the most promising technique both in research and diagnostic settings [18, 19]. Hence, relevant literature is: 1. High-resolution intracranial vessel wall MR imaging (IVW-MR imaging) [2, 3, 18, 19]. And 2. Susceptibility mapping [7, 8].

Within the context of IVW-MR imaging the correlation with the present research is the use of T2-weighted MRI [19]. The image reconstruction technique proposed here allows improved (versus T2-MRI) vessels detection and contrast enhancement. In short, it is here proposed that the task of vessel visualization through T2-weighted MRI can be enhanced through image processing. The aforementioned task is not easy to achieve through the sole use of T2-MRI. Indeed, the reconstructed image and the ICF are pivotal to the aim of improving vessel detection in T2-MRI. Moreover, it is relevant to report that IVW-MR imaging requires 3T or ultra-high-field (UHF) MRI scanners [20], while the proposed image processing technique can be used on MR acquired at low magnetic fields.

Within the context of susceptibility mapping the technique here proposed does not make use of maximum intensity projections (MIPs), neither minimum intensity projections (mIPs) [7] and it works with a single 2D MR image. MIPs and mIPs are effective in displaying contiguous veins, however, they introduce approximations. The approximations are determined because only the hypodense structures are displayed by mIPs and only the hyper dense structures are displayed by MIPs. Hence, to create 3D maps of the veins of the brain it may be preferred to work with one 2D image slice at time, likewise indicated by this research. Moreover, as recent research suggests, susceptibility mapping algorithms suffers from the diversity of solutions implemented to solve the field-to-source inverse problem, which is related to accurate estimation of the susceptibility

from MRI phase data [21]. On the other hand, the present research uses MR data to enforce high pass filtering, which is indeed: 1. The effect of calculation of ICF on MR image. And, 2. The effect of reconstructed image after fusing ICF with MR. High pass filtering might be suffering though of artefactual peaks (false "ripples") in the signal-image or by insufficient background removal. This happens for instance when high pass filtering phase images to be used in SWI [22].

4. Conclusion

It is possible through use of ICF and reconstructed image to improve vessels detail detection in T2-MRI and to make contrast enhancement in T2-MRI and MRA. Cautiously, it needs to be reminded that high pass filtering characteristics of ICF remains competitive when compared to high pass filtering obtained through the reconstructed image, and the two of them are quite similar. A good use of ICF and reconstructed image is the two of them together versus one preferred to the other one.

Acknowledgements

The author expresses sincere gratitude to Dr. Dimitar Veljanovski and Dr. Filip A. Risteski because of the availability of the MR images and also to Professor Ustijana Rechkoska Shikoska for the help provided to coordinate the human resources. Dr. Dimitar Veljanovski and Dr. Filip A. Risteski are affiliated with the Department of Radiology, General Hospital 8-mi Septemvri, Boulevard 8th September, Skopje, 1000, Republic of North Macedonia. Professor Ustijana Rechkoska Shikoska is affiliated with the University of Information Science and Technology (UIST), Partizanska BB, Ohrid, 6000, Republic of North Macedonia.

Declarations

Funding: No funding was received to support this research.

Conflicts of interest/Competing interests: None.

Availability of data and material: Data is freely available to the public upon request.

Code availability: Software is freely available to the public upon request.

Ethics approval, Consent to participate and Consent for publication: MRI acquisition was consented and approval was obtained from subjects to use the images for research after the administration of written consent. The research protocol of MRI data acquisition was were approved by the Department of Radiology, General Hospital 8-mi Septemvri, Boulevard 8th

September, Skopje, 1000, Republic of North Macedonia. This study was conducted according to principles expressed in the 1964 Declaration of Helsinki. The author of this article, Carlo Ciulla, provided the Magnetic Resonance Angiography (MRA).

References

1. Choi YJ, Jung SC, Lee DH. Vessel wall imaging of the intracranial and cervical carotid arteries. Journal of Stroke. 2015;17(3):238-55.

2. Mandell DM, Mossa-Basha M, Qiao Y, Hess CP, Hui F, Matouk C, Johnson MH, Daemen MJ, Vossough A, Edjlali M, Saloner D. Intracranial vessel wall MRI: principles and expert consensus recommendations of the American Society of Neuroradiology. American Journal of Neuroradiology. 2017;38(2):218-29.

3. Obusez EC, Hui F, Hajj-Ali RA, Cerejo R, Calabrese LH, Hammad T, Jones SE. High-resolution MRI vessel wall imaging: spatial and temporal patterns of reversible cerebral vasoconstriction syndrome and central nervous system vasculitis. American Journal of Neuroradiology. 2014;35(8):1527-32.

4. Li M, Hu J, Miao Y, Shen H, Tao D, Yang Z, Li Q, Xuan SY, Raza W, Alzubaidi S, Haacke EM. In vivo measurement of oxygenation changes after stroke using susceptibility weighted imaging filtered phase data. PloS one. 2013;8(5):e63013.

5. Swartz RH, Bhuta SS, Farb RI, Agid R, Willinsky RA, Butany J, Wasserman BA, Johnstone DM, Silver FL, Mikulis DJ. Intracranial arterial wall imaging using high-resolution 3-tesla contrast-enhanced MRI. Neurology. 2009;72(7):627-34.

6. Haacke EM, Xu Y, Cheng YC, Reichenbach JR. Susceptibility weighted imaging (SWI). Magnetic Resonance in Medicine. 2004;52(3):612-8.

7. Haacke, E.M., Tang, J., Neelavalli, J. and Cheng, Y.C.N. Susceptibility mapping as a means to visualize veins and quantify oxygen saturation. Journal of Magnetic Resonance Imaging. 2010;32(3):663-76.

8. Liu C, Li W, Tong KA, Yeom KW, Kuzminski S. Susceptibility-weighted imaging and quantitative susceptibility mapping in the brain. Journal of Magnetic Resonance Imaging. 2015;42(1):23-41.

9. Li W, Liu C, Duong TQ, van Zijl PC, Li X. Susceptibility tensor imaging (STI) of the brain. NMR in Biomedicine. 2017;30(4):e3540.

10. Jeong Y, Hwang HS, Na K. Theranostics and contrast agents for magnetic resonance imaging. Biomaterials Research. 2018;22(1):20.

11. Barisano G, Sepehrband F, Ma S, Jann K, Cabeen R, Wang DJ, Toga AW, Law M. Clinical 7 T MRI: Are we there yet? A review about magnetic resonance imaging at ultra-high field. The British Journal of Radiology. 2019;91:20180492.

12. Reichenbach, JR., Venkatesan R, Schillinger DJ, Kido DK, Haacke, EM. Small vessels in the human brain: MR venography with deoxyhemoglobin as an intrinsic contrast agent. Radiology. 1997;204(1):272-7.

13. Ciulla C. Intensity-curvature functional-based filtering in image space and in k-space: Applications in magnetic resonance imaging of the human brain. High Frequency. 2019;2(1):48-60.

14. Ciulla C. The use of the intensity-curvature measurement approaches: Applications in magnetic resonance imaging of the human brain. Engineering Reports. 2019;1(5): e12063.

15. Ciulla C, Agyapong G. Intensity-curvature functional based digital high pass filter of the bivariate cubic B-spline model polynomial function. Visual Computing for Industry, Biomedicine, and Art. 2019;2(9).

16. Ciulla C, Rechkoska US, Veljanovski D, Risteski, FA. Intensity-curvature highlight of human brain magnetic resonance imaging vasculature. Int. J. Modelling, Identification and Control. 2018;29(3):233-43.

17. Yahaya F. Edge finding in magnetic resonance imaging applications: the calculation of the first order derivative of two dimensional images, Int. J. Applied Pattern Recognition. 2017;4(3):226-45.

18. Bhogal P, Navaei E, Makalanda HL, Brouwer PA, Sjöstrand C, Mandell DM, Lilja A. Intracranial vessel wall MRI. Clinical Radiology. 2016;71(3):293-303.

19. de Havenon A, Chung L, Park M, Mossa-Basha M. Intracranial vessel wall MRI: a review of current indications and future applications. Neurovascular Imaging. 2016;2(1):10.

20. Lindenholz A, van der Kolk AG, Zwanenburg JJ, Hendrikse J. The use and pitfalls of intracranial vessel wall imaging: how we do it. Radiology. 2018;286(1):12-28.

21. Langkammer C, Schweser F, Shmueli K, Kames C, Li X, Guo L, Milovic C, Kim J, Wei H, Bredies K, Buch S. Quantitative susceptibility mapping: report from the 2016 reconstruction challenge. Magnetic Resonance in Medicine. 2018;79(3):1661-73.

22. Ishimori Y, Monma M, Kohno Y. Artifact reduction of susceptibility-weighted imaging using a short-echo phase mask. Acta Radiologica. 2009;50(9):1027-34.